

GUIDE-VAE: Advancing Data Generation with User Information and Pattern Dictionaries

Kutay Bölüt, Simon H. Tindemans

Abstract—Generative modelling of multi-user datasets has become prominent in science and engineering. Generating a data point for a given user requires employing user information, and conventional generative models, including variational autoencoders (VAEs), often ignore that. This paper introduces GUIDE-VAE, a novel conditional generative model that leverages user embeddings to generate user-guided data. By allowing the model to benefit from shared patterns across users, GUIDE-VAE enhances performance in multi-user settings, even under significant data imbalance. In addition to integrating user information, GUIDE-VAE incorporates a pattern dictionary-based covariance composition (PDCC) to improve the realism of generated samples by capturing complex feature dependencies. While user embeddings drive performance gains, PDCC addresses common issues such as noise and over-smoothing typically seen in VAEs.

The proposed GUIDE-VAE was evaluated on a multi-user smart meter dataset characterized by substantial data imbalance across users. Quantitative results show that GUIDE-VAE performs effectively in both synthetic data generation and missing record imputation tasks, while qualitative evaluations reveal that GUIDE-VAE produces more plausible and less noisy data. These results establish GUIDE-VAE as a promising tool for controlled, realistic data generation in multi-user datasets, with potential applications across various domains requiring user-informed modelling.

Index Terms—Covariance structure, generative modelling, multi-user datasets, user embedding, variational autoencoders

I. INTRODUCTION

The landscape of generative artificial intelligence grows at an ever-increasing pace like never seen before. The underlying generative models get larger in size and capacity every year to generate novel content (text, images, audio, etc.) with a close-to-human-level performance, if not better. Beyond content creation, generative models are now being leveraged by scientists, engineers, and businesses for applications such as synthetic data generation [1] and scientific discovery [2]. These applications often require some control over the generation mechanism to preserve the utility of the generated samples. Conditional generative models offer such control by introducing desired conditions to the generative process. While contemporary large language models incorporate text prompts for this purpose, the datasets from various scientific domains (measurements, logs, surveys, etc.) may require more tailored conditions [3].

The authors are with the Department of Electrical Sustainable Energy, Delft University of Technology, Mekelweg 4, 2628 CD Delft, The Netherlands.

This research was undertaken as part of the InnoCyPES project, which has received funding from the European Union’s Horizon 2020 research and innovation programme under the Marie Skłodowska-Curie grant agreement No 956433.

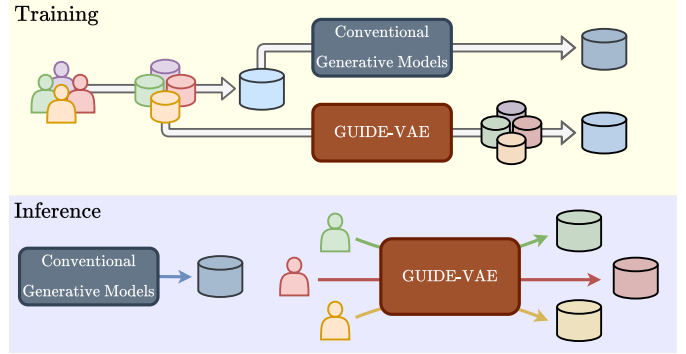


Fig. 1. Conventional generative models disregard user information during training, treating the dataset anonymously, which limits their ability to generate data for specific users during inference. GUIDE-VAE addresses this by incorporating user information in the training process, enabling control over the generated outputs for individual users.

Variational autoencoders (VAEs) [4], along with conditional VAEs (CVAEs) [5], are widely adopted generative models that use probabilistic encoders and decoders. These models extend variational inference methods through the power of deep neural networks, offering notable advantages, e.g. efficient data encoding and a strong probabilistic foundation. However, similar to many generative models, VAEs have certain limitations. One of the well-known drawbacks is that they can produce synthetic samples that lack fine-grained detail, often resulting in blurry or noisy outputs [6]. This issue is particularly striking when the dataset exhibits strong correlations between features, as seen in time-series data, where failing to capture these correlations can significantly reduce the realism of generated samples.

Multi-user datasets, such as smart meter readings [7], patient health records [8], and user interaction data from digital platforms [9], consist of records from multiple individuals, with each user contributing data that reflects their unique behaviours and preferences. These datasets are crucial for capturing user-level patterns, like individual energy consumption [10] or patient treatment responses [8], which are informative for personalized recommendations and targeted solutions. In this context, synthetic data generation enables the analysis and simulation of these trends [11]. However, modelling these datasets presents significant challenges: training separate models for each user is inefficient and impractical, while anonymizing user identities leads to a loss of control over generating the specific patterns unique to each user, as shown in Fig. 1.

One well-known data mining application parallel to multi-user datasets is topic modelling in textual data. This tech-

nique analyzes a corpus of documents, each consisting of multiple words, and models the relationships between them by assigning abstract topics to documents. Latent Dirichlet allocation (LDA) [12] is a widely used method for topic modelling, where it effectively captures the latent structure within the data. The resemblance between a document corpus and a multi-user dataset—where documents correspond to users and words to individual data records—makes the application of LDA in multi-user domains both intuitive and powerful. This analogy enables LDA to model the structure of multi-user datasets by grouping similar users based on their data characteristics. In [10], this approach is applied to smart meter data, yielding useful insights into consumer behaviour and consumption patterns. The ability of LDA to reveal such underlying patterns makes it a promising tool for extracting valuable information from multi-user datasets in diverse applications.

A. Problem Statement

This work addresses two main challenges: (i) the absence of user-specific guidance during the generative process and (ii) the lack of realism in the generated data. The following subsections delve deeper into these issues.

1) *Lack of Guidance*: Efficient application of conventional generative models to multi-user datasets remains limited. These datasets contain user-specific information, which, if overlooked, leads to synthetic data that fails to reflect individual patterns and behaviours. This problem becomes even more severe in the presence of data imbalance, where users with lower data counts are under-represented [8], and possibly hinder fairness [13]. Moreover, without incorporating user information, controlling the generative process to produce data for a specific user becomes highly challenging and may require complex, ad-hoc methods [14].

The key issue lies in the absence of a mechanism to represent user identities as mathematical objects that can be used as conditions during the generative process. Without such a representation, generative models cannot efficiently encode or utilize the user-specific information required to guide data generation. A similar problem is encountered in the neural collaborative filtering field where the user and the items they interact with are related to each other [9]. This requires representing users as inputs to neural networks. However, this is generally done by using one-hot encoding, which limits the scalability and generalization.

To address this challenge, user embeddings that represent users based on their data offer a promising solution. These embeddings map users into a metric space where their similarities can be quantified [10], allowing the generative model to condition on these embeddings and generate data that reflects user-level patterns. However, conventional generative models do not employ such an approach, leaving a gap in their ability to accurately condition on user identities. The absence of this capability not only limits the precision of the generated data but also hinders the potential for inter-user knowledge transfer, which could improve both the quality and variability of the synthetic outputs.

2) *Lack of Realism*: VAEs utilize two probabilistic distributions during the generative process: the likelihood and the prior distributions. A commonly used likelihood distribution is the multivariate Gaussian with a diagonal covariance matrix, where the model assumes independence between features for a given latent variable [4]. While this assumption simplifies the modelling process, it often leads to poor sample quality. Specifically, by treating features as independent, VAEs tend to produce noisy data, as it falls outside the manifold of the original data [15]. This problem is particularly significant for time-series data generation, where capturing correlations between sequential data points is crucial for preserving informative patterns, such as peaks and cycles in energy consumption patterns.

A common workaround to improve sample quality is using the mean vector as the generated sample, which often results in overly smooth (“blurry”) outputs. These two options for the generative process impose a significant limitation on VAEs in generating realistic data, especially for applications that require fine-grained detail.

One natural question arises: why not employ full covariance matrices to better capture feature dependencies? While full covariance matrices could, in theory, solve this issue, they introduce several practical challenges:

- *Parameterization*: Full covariance matrices are more difficult to parameterize as an output of a neural network, requiring elaborate mechanisms to ensure positivity.
- *Singularity*: Full covariance matrices are prone to singular solutions, particularly during training, making them harder to constrain compared to their diagonal variants.

In [15] and [16], these problems are addressed by using Cholesky and low-rank decompositions, respectively. However, these require either sparsity assumptions [15] or regularization on the objective function [16], which limits the representative power. These challenges have limited the adoption of full covariance matrices in VAEs, leaving a gap in the literature and hindering progress toward generating high-quality, realistic synthetic data, particularly in fields that require accurate temporal or feature-based dependencies.

B. Main Contributions

In this work, we introduce **Generalized User-Informed Dictionary Enhanced VAE (GUIDE-VAE)**, a novel framework that advances generative modelling for multi-user datasets through four main contributions: (i) a user-guided data generation process enabled by user embeddings, (ii) a novel covariance structure (PDCC) that enhances sample realism, and the applications of GUIDE-VAE for (iv) synthetic multi-user dataset generation and (iv) missing record imputation under data imbalance.

- (i) **User embeddings for generative modelling**: We propose a novel methodology to condition generative models on user identities by employing user embeddings. LDA is utilized to create automated embeddings, transforming users into vectors in a metric space that captures the similarities between them. These embeddings serve as conditions in a conditional generative model (in this

case, a CVAE), enabling a *user-guided* data generation process. This model (GUIDE-VAE) allows the model to generate data specific to individual users. To the best of our knowledge, this is the first instance of data-driven user-information integration being applied to generative modelling.

- (ii) **Novel covariance structure and improved realism:** We introduce a new covariance matrix construction method, PDCC, which is applied in the GUIDE-VAE likelihood distribution to enhance sample realism. By learning *dependency patterns* among features, PDCC effectively mitigates the noisy sample issue commonly encountered in VAEs while ensuring positive definiteness and avoiding singularity problems without sparsity and regularization assumptions. This method maintains generalizability and offers a scalable solution for realistic data generation. To the best of our knowledge, this is the first time such a full covariance matrix parameterization has been successfully implemented in this context.
- (iii) **Synthetic multi-user time series data generation:** We propose a novel approach to synthetic data generation that explicitly addresses the multi-user nature of datasets. GUIDE-VAE enables the generation of realistic time-series data across multiple users by conditioning on user embeddings, significantly improving modelling performance compared to conventional unguided CVAEs. This approach offers a new solution for generating diverse and realistic synthetic time series data tailored to individual users, addressing a key limitation in current generative models by incorporating the multi-user aspect.
- (iv) **Inter-user information transfer and imputation:** We introduce the problem of missing record imputation in multi-user datasets under data imbalance, where the number of missing records varies among users. GUIDE-VAE leverages inter-user knowledge transfer through embeddings to mitigate this issue, utilizing data from similar users to improve imputation accuracy. As a result, the model effectively handles users with fewer data points, naturally improving imputation performance without being explicitly designed to address data imbalance.

We evaluated GUIDE-VAE using a multi-user smart meter dataset to demonstrate its performance and added benefits. To simulate the data imbalance, we created an enrollment model where users enrol in the data collection system randomly late, reflecting real-world conditions. In this use case, the dataset owner (e.g., a utility company) aims to (1) create a synthetic version of the dataset and (2) complete the dataset by imputing the missing records for late-enrolling users.

II. PRELIMINARIES

A. Multi-user Time-series Profiles

We consider datasets which consist of a collection of regularly and synchronously sampled time series profile data from multiple sources (users, for this study), as can be seen in Fig. 2. We denote the u^{th} user’s dataset as $\mathbb{X}_u = \{\mathbf{x}_{un}\}_{n=1}^{N_u}$ where $\mathbf{x}_{un} = \left[x_{un}^{(t)} \right]_{t=1}^T \in \mathcal{X}^T \subseteq \mathbb{R}^T$. Here, N_u is the number of recorded profiles, and T is the profile length,

e.g. $T=24$ corresponds to daily profiles for hourly sampled time series. These *user datasets* can be pooled (anonymized) under $\mathbb{X} = \{\mathbf{x}_i | \mathbf{x}_i \in \bigcup_{u=1}^U \mathbb{X}_u\}$ where U is the total number of users. Note that each element \mathbf{x}_i has a one-to-one correspondence to a user-indexed data point \mathbf{x}_{un} .¹ We also assume that pieces of contextual information \mathbf{c}_{un} assigned to each data point \mathbf{x}_{un} , which can be used as conditions for the generative modelling as described in following sections.

B. Latent Dirichlet Allocation

LDA [12] is a variational method for topic discovery applied to collections of discrete data. It is essentially a multi-level Bayesian model that exploits the occurrence frequencies of data classes (words) in data collections (documents) to cluster both of these as mixture models. The mixture components are conventionally named as *topics*, and a topic vector can be assigned to a given document using the posterior distribution of the model. In our context, LDA will allow us to discover latent structures in multi-user time-series data, enabling us to model user profiles as distributions over latent topics.

Here, we define a dataset consisting of U documents $\mathbb{W} = \{\mathbb{W}_u\}_{u=1}^U$ where $\mathbb{W}_u = \{w_{un}\}_{n=1}^{N_u}$, and each $w_{un} \in \{1, \dots, W\}$ represents a discrete variable out of W classes.² Since this study utilizes only the topics assigned to documents, the originally proposed Bayesian model in [12] is reduced to a two-level hierarchy as

$$\begin{aligned}
 p(\mathbb{W}, \theta, \beta; \alpha, \eta) &= \prod_{k \in [K]} \prod_{u \in [U]} p(\mathbb{W}_u | \theta_u, \beta_k) p(\theta_u; \alpha) p(\beta_k; \eta) \\
 &= \prod_k \prod_u \mathcal{M}(\mathbb{W}_u | \sum_{k \in [K]} \theta_u^{(k)} \beta_k; N_u) \mathcal{D}(\theta_u; \alpha) \mathcal{D}(\beta_k; \eta)
 \end{aligned} \tag{1}$$

where K is the number of topics. Here, each $\theta_u \in \Delta^{K-1}$ represents the document-topic weights for the u^{th} document and is *Dirichlet distributed* with concentration parameter $\alpha > 0$. Similarly, the word weights for each topic k , $\beta_k \in \Delta^{W-1}$, is *Dirichlet distributed* with the concentration parameter $\eta > 0$. Lastly, each document \mathbb{W}_u has a *multinomial distribution* with N_u number of trials and an event probabilities vector of $\sum_k \theta^{(k)} \beta_k \in \Delta^{W-1}$.

Intuitively, this model describes a generative process to create documents as bags of words according to some latent topics. In order to reverse this process to find the corresponding topic weights of a given document, one must acquire the posterior distribution $p(\theta_u | \mathbb{W}_u; \alpha, \eta) \propto p(\mathbb{W}_u | \theta_u; \eta) p(\theta_u; \alpha)$ which is inherently intractable. Instead, using variational inference, this posterior can be approximated as $q(\theta_u; \gamma_u) = \mathcal{D}(\theta_u; \gamma_u)$ by estimating the parameter γ_u after the convergence of the proposed expectation-maximization algorithm in [12]. This variational inference from documents to the posterior parameters γ_u is depicted as the core of the user embedding pipeline visualized in Fig. 2.

¹One mapping can be $i = n + \sum_{u'=0}^{u-1} N_{u'}$, $N_0 = 0$.

²Conventionally, these classes correspond to actual words. We keep them as integers for mathematical convenience. Note that the magnitude of these integer values does not convey any information.

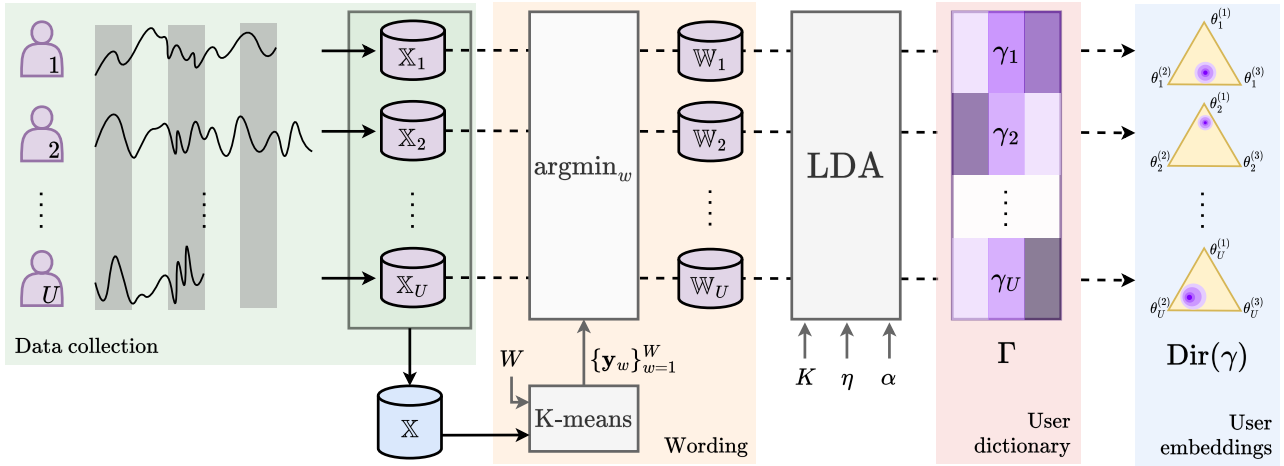


Fig. 2. The user embedding framework for multi-user time-series datasets. Users’ time-series data are segmented into profiles and clustered using k -means. These clusters are treated as words, and user datasets are treated as documents for LDA. After training, LDA produces a user dictionary Γ , where each element corresponds to the parameters of a Dirichlet distribution, serving as user embeddings.

C. Variational Autoencoders

VAEs [4] are generative models that extend the variational Bayesian inference methodology to realms of deep learning and they operate by using three key distributions: the likelihood $p_\psi(\mathbf{x}|\mathbf{z})$, the approximate posterior $q_\phi(\mathbf{z}|\mathbf{x})$, and the prior $p(\mathbf{z})$. Here, \mathbf{z} is a latent variable while \mathbf{x} is an observed one. Even though the family selection of these distributions is very flexible, it is common to choose the distributions as multivariate normal distributions as follows:

$$p_\psi(\mathbf{x}|\mathbf{z}) = \mathcal{N}(\mathbf{x}; \mu = f_\psi^\mu(\mathbf{z}); \Sigma = \text{diag}(f_\psi^\sigma(\mathbf{z}))), \quad (2)$$

$$q_\phi(\mathbf{z}|\mathbf{x}) = \mathcal{N}(\mathbf{z}; \mu = f_\phi^\mu(\mathbf{x}); \Sigma = \text{diag}(f_\phi^\sigma(\mathbf{x}))), \quad (3)$$

$$p(\mathbf{z}) = \mathcal{N}(\mathbf{z}; \mu = \mathbf{0}, \Sigma = \mathbf{I}). \quad (4)$$

Here, the neural networks $\{f_\psi^\mu, f_\psi^\sigma\}$ and $\{f_\phi^\mu, f_\phi^\sigma\}$ form the VAE’s decoder and encoder neural networks, whose parameters are collected in ψ and ϕ , respectively. After setting up the distributions and neural networks, the VAE can be trained to maximize the evidence lower bound (ELBO) as

$$\begin{aligned} \psi^*, \phi^* &= \arg \max_{\psi, \phi} \sum_{\mathbf{x}_i \in \mathbb{X}} \mathbb{E}_{q_\phi(\mathbf{z}|\mathbf{x}_i)} \left[\log \frac{p_\psi(\mathbf{x}_i|\mathbf{z})p(\mathbf{z})}{q_\phi(\mathbf{z}|\mathbf{x}_i)} \right] \\ &= \arg \max_{\psi, \phi} \sum_{\mathbf{x}_i \in \mathbb{X}} \frac{\sum_l^{N^{\text{MC}}} \log p_\psi(\mathbf{x}_i|\hat{\mathbf{z}}_{il})}{N^{\text{MC}}} - \text{D}_{\text{KL}}(q_\phi(\mathbf{z}|\mathbf{x}_i)||p(\mathbf{z})) \end{aligned} \quad (5)$$

where $\hat{\mathbf{z}}_{il} \sim q_\phi(\mathbf{z}|\mathbf{x}_i)$ is the l^{th} sample of the posterior distribution for a given data point \mathbf{x}_i and N^{MC} is the number of Monte Carlo samples to approximate $\mathbb{E}_{q_\phi(\mathbf{z}|\mathbf{x}_i)}[\log p_\psi(\mathbf{x}_i|\mathbf{z})]$.

Since the ELBO objective is a lower bound for the exact log-likelihood $\log p_\psi(\mathbb{X})$ [4], maximizing it equips the VAE with two main functionalities. Firstly, one can take a sample from the marginal distribution model, $\hat{\mathbf{x}} \sim p_\psi(\mathbf{x})$, through ancestral sampling as $\hat{\mathbf{x}} \sim p_\psi(\mathbf{x}|\hat{\mathbf{z}})$, $\hat{\mathbf{z}} \sim p(\mathbf{z})$, since $p_\psi(\mathbf{x}) = \mathbb{E}_{p(\mathbf{z})}[p_\psi(\mathbf{x}|\mathbf{z})]$. This provides the ability to generate unlimited data points and create synthetic datasets. Secondly, the latent variables conditioned on observed data through the posterior distribution can be used in various applications,

such as dimensionality reduction and clustering. This study is mainly interested in the first functionality of the VAEs, and we invite researchers to investigate the effects of the proposed methods on the latent variables.

1) *Conditional variational autoencoders*: One natural extension of VAEs is their conditional counterparts, CVAEs [5]. These generative models aim to model the conditional distribution $p_\psi(\mathbf{x}|\mathbf{c})$, instead of $p_\psi(\mathbf{x})$ as in conventional VAEs as explained above. These conditions, \mathbf{c} , are generally known aspects of the random variables, such as labels and assigned contextual information pieces. Thanks to this additional information, CVAEs can learn to generate data belonging to a given condition, $\hat{\mathbf{x}}|\mathbf{c} \sim p_\psi(\mathbf{x}|\mathbf{c})$, which provides additional control on the synthetic data generation process.

Introducing the conditions into the VAEs requires only a minimal adjustment to the setting and training. Derivation of ELBO remains the same except the structures of the distributions which take the form $p_\psi(\mathbf{x}|\mathbf{z}, \mathbf{c})$ and $q_\phi(\mathbf{z}|\mathbf{x}, \mathbf{c})$.³ Thus, after concatenating the conditions into the observed and latent variables as inputs of encoder and decoder networks, respectively, (5) can be used for the CVAE training. The corresponding overall structure is depicted in Fig. 3.⁴

III. METHODOLOGY

The proposed GUIDE-VAE framework combines two core components: user embeddings extracted via LDA for conditioning on user-specific patterns and a CVAE enhanced with PDCC to capture feature dependencies and improve realism. Together, these components enable GUIDE-VAE to generate personalized, high-quality time-series data.

³Theoretically, the prior also takes the form of $p(\mathbf{z}|\mathbf{c})$, but it usually left untouched due to the extra amortization load.

⁴Note that this structure applies only to training. During the inference for synthetic data generation, one does not aim to reconstruct a data point but to generate it. This means applying ancestral sampling together with the conditions as $\hat{\mathbf{x}}|\mathbf{c} \sim p_\psi(\mathbf{x}|\hat{\mathbf{z}}, \mathbf{c})$, $\hat{\mathbf{z}} \sim p(\mathbf{z})$.

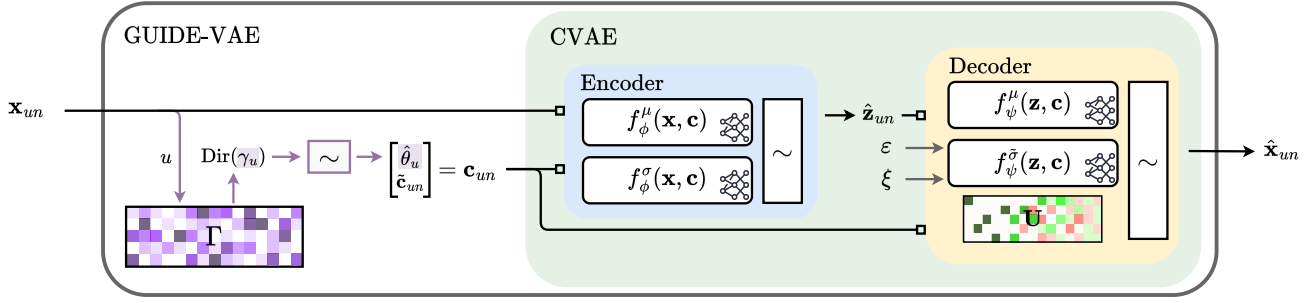


Fig. 3. Overall computational diagram of GUIDE-VAE. GUIDE-VAE is a CVAE-based model enhanced with a learnable pattern dictionary for PDCC, which captures feature dependencies for improved realism. The user of the data point is selected from the user dictionary, and a sample from the corresponding probabilistic embedding is concatenated with auxiliary conditions (e.g., metadata or timestamps) and applied to both the encoder and decoder.

A. Guidance: LDA-based user-embedding

As it is described in Section II-B, LDA assigns topic weights to each word in a vocabulary and uses these assignments to calculate the posterior of a given document. Therefore, after training it, LDA can be used to map documents to Dirichlet distributions. This resembles the desired user-embedding scheme since documents are also non-mathematical entities with varying sizes of (text-based) datasets. Following this resemblance, LDA can also be applied to multi-user time series datasets. However, most time series datasets do not consist of words or discrete features in a finite domain, e.g. categories. Instead, they tend to have records in continuous domains. In [10], a data preprocessing pipeline is proposed to apply LDA to a non-textual time series dataset. This “wording” process enables the continuous time series data to be mapped into a discrete space, making it compatible with LDA’s document-word structure.

The wording consists of three steps, as depicted in Fig. 2. First, k -means clustering is applied to the pooled dataset \mathbb{X} described in Section II-A. This results in W cluster centres corresponding to the “wording granularity”. Then, the user time series profiles \mathbf{x}_{un} are replaced with the respective cluster labels to which they are assigned to, i.e. $w_{un} = \arg \min_w \|\mathbf{x}_{un} - \mathbf{y}_w\|$ where $\mathbf{y}_w \in \mathcal{X}^T$ represent the w^{th} cluster centre and $w \in \{1, \dots, W\}$. Consequently, each user dataset consists of cluster labels that are interpreted as words, and “user documents” are formed as $\mathbb{W}_u = \{w_{un}\}_{n=1}^{N_u}$.

Treating users as documents allows LDA to generate approximate posterior distributions for each user dataset, $\mathcal{D}(\theta_u; \gamma_u)$, where $\gamma_u \in \mathbb{R}_+^K$ can be calculated iteratively using the document and the prior parameters as mentioned in Section II-B. Consequently, the resulting distribution is treated as the user embedding that is aimed for, and the concentration parameters of these embeddings can be collected in a “user dictionary” $\Gamma = \{\gamma_u\}_{u=1}^U$ as shown in Fig. 2. Note that, unlike [10], the mean of the distribution, $\mathbb{E}[\theta_u] = \frac{\gamma_u}{\sum_k \gamma_u^{(k)}}$, is not used as the embedding since the remaining moments (or simply the shape) of the distribution also contain information. For instance, users with low data counts result in distributions with larger variances, and employing only the mean values of these distributions neglects this inherited uncertainty.

Embedding users as distributions introduces the challenge of applying these as conditions in mathematical models like

CVAEs. This can be done by finding a kernel mean embedding [17] of the Dirichlet distribution and mapping the user distributions into vectors. However, this is mathematically cumbersome and outside of this study’s scope. Instead, a sampling-based alternative method is proposed where each distribution is represented with a collection of “user vectors” $\hat{\theta}_{us} \sim \text{Dir}(\gamma_u)$. This sampling-based approach not only simplifies the process but also captures the variability and uncertainty inherent in user distributions, making it a practical choice for large-scale datasets. In practice, if the users are revisited indefinitely like in a neural network training, user vectors can be sampled per visit and storing only the user dictionary Γ is sufficient.

B. Realism: Likelihood distributions using PDCC

We propose a novel matrix composition method, termed PDCC, to parameterize the full covariance matrix of the GUIDE-VAE’s likelihood distribution. This section first gives the intuition behind PDCC, then its theoretical foundation, and lastly, the useful properties that come with it.

1) *Intuition:* PDCC can be interpreted as a pattern-dictionary scheme where the features of random variables correlate by mapping high-dimensional uncorrelated noise. To elaborate, let us investigate the sampling scheme of a multivariate Gaussian distribution with a diagonal covariance matrix, $\Sigma = \text{diag}(\sigma)$ and zero mean vector, $\mu = \mathbf{0}$. After having T i.i.d. samples from a unit normal distribution, $\{\hat{\epsilon}_t\}_{t=1}^T \stackrel{T}{\sim} \mathcal{N}(0, 1)$, the final sample taken from the distribution can be acquired as $\hat{\mathbf{x}} = [\sigma^{(t)} \hat{\epsilon}_t]_{t=1}^T$, which can be represented as

$$\hat{\mathbf{x}} = \sum_{t=1}^T \text{OneHot}(t, T) \sigma^{(t)} \hat{\epsilon}_t = \mathbf{I} \Sigma [\hat{\epsilon}_t]_t \quad (6)$$

where $\text{OneHot}(t, T)$ is a T dimensional one-hot-vector whose all elements are 0 except $\text{OneHot}(t, T)^{(t)} = 1$. This one-hot representation shows the uncoupled nature of the progression from the noise samples $\{\hat{\epsilon}_t\}$ to $\hat{\mathbf{x}}$, which aligns with the independence of the features.

Now, let us denote a new sampling mechanism as

$$\hat{\mathbf{x}} = \sum_{v=1}^V \mathbf{u}_v \tilde{\sigma}^{(v)} \hat{\epsilon}_v = \mathbf{U} \tilde{\Sigma} [\hat{\epsilon}_v]_v \quad (7)$$

where $\{\hat{\epsilon}_v\}_{v=1}^V \overset{V}{\sim} \mathcal{N}(0, 1)$ and $V > T$. Please note the resemblance to (6) but two main differences: The one-hot vectors are replaced with \mathbf{u}_v , and the number of elements to be summed increased from T to V . The former implies that each noise sample can now affect all the features through the *pattern vectors*, \mathbf{u}_v , that represent dependency patterns between the features. On the other hand, the latter implies that, unlike vanilla covariance matrix compositions, the number of these vectors is not limited by T , which creates the opportunity to employ (and learn) a large *pattern dictionary*, defined as $\mathbf{U} = [\mathbf{u}_v^\top]^\top \in \mathbb{R}^{T \times V}$. This dictionary matrix maps high-dimensional uncorrelated noise vector $[\hat{\epsilon}_v]$ to a lower-dimensional one. The resulting mapping can flourish arbitrary correlations as it will be introduced theoretically in the rest of the subsection.

2) *Definition*: First, let $\tilde{\sigma} = [\tilde{\sigma}^{(v)}]_{v=1}^V \in \mathbb{R}_+^V$ represent the *auxiliary standard deviations* in a higher dimensional space ($V > T$). Next, let us define a transformation matrix $\mathbf{U} = [\mathbf{u}_v^\top]^\top \in \mathbb{R}^{T \times V}$, where each column $\mathbf{u}_v \in \mathbb{R}^T$ has a unit norm, i.e. $\|\mathbf{u}_v\| = 1 \forall v$. Lastly, let $\xi \in \mathbb{R}_+$ represent the *base variance*. Having these three components, a covariance matrix $\Sigma \in \mathbb{R}_+^{T \times T}$ can be composed as

$$\Sigma = \mathbf{U} \tilde{\Sigma} \mathbf{U}^\top + \xi \mathbf{I} \quad (8)$$

where $\tilde{\Sigma} = \text{diag}(\tilde{\sigma})^2$. Note that the composition $\mathbf{U} \tilde{\Sigma} \mathbf{U}^\top$ is positive definite as long as $\text{rank}(\mathbf{U}) = T$, and positive semi-definite else. It can be proved easily using positive definiteness and matrix rank properties. In either way, (8) ensures Σ is always positive definite due to $\xi > 0$.

3) *Properties*: Motivated by the problem definition in I-A2, we claim that PDCC provides the following properties.

- **Constrainability** - PDCC is spectrally constrainable for avoiding singularities: Let $\{\tilde{\lambda}_t\}_{t=1}^T$ represent the eigenvalues of $\mathbf{U} \tilde{\Sigma} \mathbf{U}^\top$ where $\tilde{\lambda}_t > 0 \forall t$. Therefore, by the definition of eigenvalue decomposition, the eigenvalues of Σ are $\{\lambda_t | \lambda_t = \tilde{\lambda}_t + \xi\}_{t=1}^T$, which makes them bounded from below by ξ , preventing singularity. On the other hand, likelihood calculations require inverting Σ , and this inversion fails if $\det(\Sigma) \approx 0$ despite its positivity. The constant ξ can also prevent this since $\det(\Sigma) = \prod_t \lambda_t = \prod_t (\tilde{\lambda}_t + \xi) > \xi^T$. However, note that ξ can be interpreted as an isotropic Gaussian noise (or density) added by default, hence the naming base variance. In order to preserve the realism aspect of the samples, the base variance must be kept at moderate levels, e.g. $\xi < 1$. Unfortunately, ξ^T diminishes exponentially with the increasing dimensionality, and one must sacrifice a certain level of realism to guarantee numerical stability.
- **Flexibility** - PDCC is flexible enough for capturing inter-dependencies: Every positive definite covariance matrix can be subjected to Cholesky decomposition as $\Sigma = LL^\top$ where L is a unique lower triangular matrix with positive diagonal elements. Vice versa, a valid matrix L can generate a unique covariance matrix. Therefore, it can be claimed that a covariance matrix Σ has a degree of flexibility $\frac{T(T+1)}{2}$, which is the number of lower triangular elements of L . Meanwhile, PDCC provides

$1 + VT + V$ parameters in total, which is always larger than $\frac{T(T+1)}{2}$. This can be shown easily by using basic algebraic manipulations and the inequality $T < V$. Thus, it can be concluded that PDCC offers an overparameterized way to construct any positive definite matrix. A proof for this is provided in Appendix A.

- **Parameterizability** - PDCC is efficiently parameterizable for neural network training: We propose a partial parameterization scheme for PDCC since its overparameterized nature makes it challenging to model it as the output of a neural network. In this scheme, only the auxiliary standard deviations $\tilde{\sigma}$ are related to latent variables using $f_{\psi}^{\tilde{\sigma}}(\mathbf{z})$ while the parameters of \mathbf{U} are kept as global learnable parameters, i.e. a shared dictionary. Lastly, the base variance ξ is set as a hyper-parameter due to the reasons given earlier. Consequently, the resulting likelihood distribution is represented as

$$p_{\psi, \mathbf{U}}(\mathbf{x} | \mathbf{z}) = \mathcal{N}(\mathbf{x}; \mu = f_{\psi}^{\mu}(\mathbf{z}), \Sigma = \mathbf{U} \text{diag}(f_{\psi}^{\tilde{\sigma}}(\mathbf{z}))^2 \mathbf{U}^\top + \xi \mathbf{I}). \quad (9)$$

One might question the benefit of having a dictionary with a size larger than T since the resulting covariance matrix still has a rank of T . However, because \mathbf{U} is global, latent variables can influence the generated data only through the auxiliary standard deviations. This means that \mathbf{U} must learn the most frequent patterns among the dataset. Thus, the dictionary size V allows controlling the permissible amount of fine-grained details in the generated data points.

C. GUIDE-VAE

The proposed GUIDE-VAE model is a CVAE that is enhanced with user embeddings and PDCC, as depicted in Fig. 3. Its likelihood and posterior distributions are defined as

$$p_{\psi, \mathbf{U}}(\mathbf{x} | \mathbf{z}, \mathbf{c}) = \mathcal{N}(\mathbf{x}; f_{\psi}^{\mu}(\mathbf{z}, \mathbf{c}), \mathbf{U} \text{diag}(f_{\psi}^{\tilde{\sigma}}(\mathbf{z}, \mathbf{c}))^2 \mathbf{U}^\top + \xi \mathbf{I}) \quad (10)$$

and

$$q_{\phi}(\mathbf{z} | \mathbf{x}, \mathbf{c}) = \mathcal{N}(\mathbf{z}; f_{\phi}^{\mu}(\mathbf{x}, \mathbf{c}), \text{diag}(f_{\phi}^{\sigma}(\mathbf{x}, \mathbf{c}))^2), \quad (11)$$

respectively, where $\mathbf{c} = [\hat{\theta}, \tilde{\mathbf{c}}]$ is the condition vector. This vector contains the user vector $\hat{\theta}$, sampled from the user embedding, and the auxiliary condition vector $\tilde{\mathbf{c}}$, which includes additional contextual information, such as timestamps or other relevant features. The prior distribution remains unchanged and is kept as $p(\mathbf{z}) = \mathcal{N}(\mathbf{z}; \mathbf{0}, \mathbf{I})$.

To ensure numerical stability and prevent degenerate solutions, we apply a lower bound constraint on the auxiliary standard deviations, $f_{\psi}^{\tilde{\sigma}^{(v)}}(\mathbf{z}, \mathbf{c}) > \epsilon, \forall v$. Without this constraint, there is a risk that the decoder could disregard the pattern vectors, leading the likelihood distribution to converge prematurely to $\mathcal{N}(\mathbf{x}; f_{\psi}^{\mu}(\mathbf{z}, \mathbf{c}), \xi \mathbf{I})$, thereby failing to learn meaningful patterns. By enforcing this constraint, we ensure that the decoder utilizes the pattern dictionary during training and that the pattern dictionary learns informative correlations between features.

IV. EXPERIMENTS

A. Data preparation

1) *Dataset*: The dataset used in this study consists of smart meter data collected from various electricity consumers across 47 provinces in Spain, including homes, offices, and businesses [18]. The dataset includes 25,559 customers (users) and their hourly electricity consumption measurements (kWh) collected between November 2014 and June 2022.⁵ However, since the consumers enrol the data collection system not at the same time, there is an imbalance in the dataset between the users in terms of data quantity that we want to stress in the experimentation.

This study uses a spatiotemporal subset of the entire dataset: Only the data collected from Gipuzkoa (the province with the highest data density) between June 2021 and June 2022 is included in the experiments. Also, the users who enrolled after June 2021 and who finished their enrollment before June 2022 are eliminated, i.e. only the users with at least one full year enrollment are kept. Lastly, the users that constantly consume 0 kWh or show negative consumption at least once are eliminated, too. These resulted in a dataset with $U=6830$ users and $N_u=365$ daily ($T=24$) profiles for each, which equates to a total number of $\sim 2.5M$ records.

As stated in Section I-B, it is desired to mitigate the user imbalance problem in a multi-user dataset. This problem is already apparent in the data collection in [18], and the sub-dataset created above can be used to simulate the late enrolment problem. Note that this simulated dataset has ground truths for the missing records, unlike the original one.

In order to create an artificial missingness, the data of each user's first days are "amputated" randomly, corresponding to randomly late enrolments. For this purpose, the beta-binomial distribution with the probability mass function (pmf)

$$P(M = m; a, b, n) = \binom{n}{m} \frac{\mathcal{B}(m-a, m-k+b)}{\mathcal{B}(a, b)} \quad (12)$$

is employed to take i.i.d. late enrolment samples for each user, i.e. $N_u = 365 - M_u$ where $M_u \sim \text{BetaBinom}(a, b, n)$, $\forall u$. Here, \mathcal{B} is the Beta function, $a > 0$ and $b > 0$ are shape parameters, and n represent the length of the integer support $m \in \{0, 1, \dots, n\}$. In this study, the parameters n and a are set to 365 and 0.85, respectively; thus, the "severity of missingness" is controlled by the parameter b . In Fig. 4, the pmfs generated by different b values are plotted in a logarithmic scale. Note that the mean of the distribution is calculated as $\mathbb{E}[M] = \frac{na}{a+b}$ and it is inversely proportional to b ; hence it is named as *data availability parameter*. A depiction of a possible missingness pattern is given in Fig. 5.

2) *Preprocessing*: Energy consumption data tends to have occasional peaks, and these cause a heavy tail in the data distribution, as can be seen in Fig. 6a. The conventional way to deal with such heavy-tailed data is by applying a logarithmic transform. However, energy consumption data is inherently "zero-inflated", meaning that there are data instances (in time) that have no energy consumption. These exact zero values

⁵The dataset has two versions: raw with missing values and the imputed one. This study uses the imputed version.

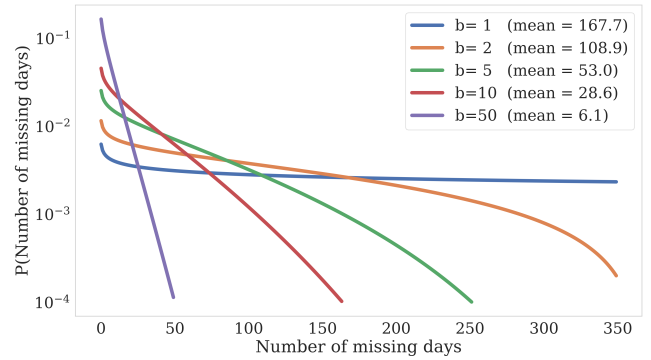


Fig. 4. The pmf of beta-binomial distribution ($n=365$, $a=0.85$) in logarithmic scale for different b values.

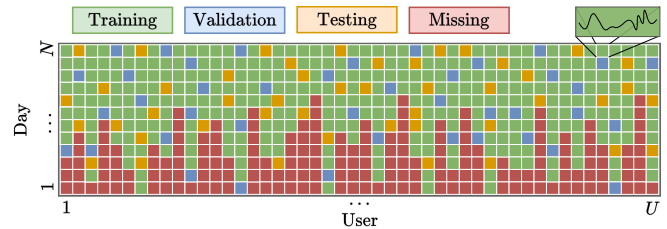


Fig. 5. The data splitting scheme used in experimentation. A full dataset where each user has an equal number of profiles first amputated according to beta-binomial distribution, and these are reserved in the missing set (in red). The remaining randomly split into training (green), validation (blues) and testing (yellow) sets.

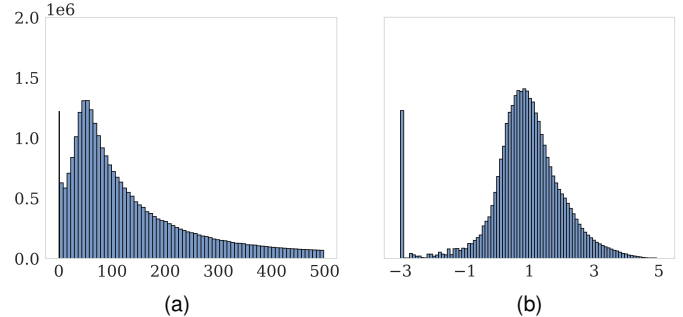


Fig. 6. The distributions of (a) measurements (in Wh) in the dataset and (b) the zero-preserved log-normalization ($h_0=-3$, $h_+=1$) applied to them.

prevent the direct use of the logarithmic transformation. To mitigate this, we propose a novel scaling technique called zero-preserved log-normalization.

Definition 1 (Zero-preserved log-normalization). Given a non-negative scalar dataset $\mathbb{X} = \{x_n\}_{n=1}^N$, $x_i \in \mathbb{R}_{\geq 0} \forall i$, two index sets can be created as $\mathbb{I}_+ = \{i | x_i > 0, x_i \in \mathbb{X}\}$ and $\mathbb{I}_0 = \{i | x_i = 0, x_i \in \mathbb{X}\}$, representing the indices of positive and zero valued elements in \mathbb{X} , respectively. Zero-preserved log-normalization transforms the dataset \mathbb{X} into $\bar{\mathbb{X}} = \{\bar{x}_i\}$ where

$$\bar{x}_i = f^{\text{ZPLN}}(x_i; m, s, h_+, h_0) = \begin{cases} \frac{\log x_i - m}{s} + h_+, & i \in \mathbb{I}_+ \\ h_0, & i \in \mathbb{I}_0 \end{cases} \quad (13)$$

Here, $m = \frac{1}{|\mathbb{I}_+|} \sum_{i \in \mathbb{I}_+} \log x_i$, $s^2 = \frac{1}{|\mathbb{I}_+|} \sum_{i \in \mathbb{I}_+} (\log x_i - m)^2$, and h_+ is a shifting constant of choice.

The constants h_0 and h_+ are used to provide an effective separation between zero and positive consumption values.⁶ The resulting data distribution after applying zero-preserved log-normalization, with $h_0=-3$ and $h_+=1$, to the dataset is given in Fig. 6b, and the desired log-normality can easily be spotted. Also, choosing h_0 smaller enough than h_+ makes the inverse transformation robust to small deviations around h_0 , i.e. if $\bar{x} = h_0 \pm \delta$ and $h_+ \gg h_0 + \frac{m}{s} + \delta$, then $x = \exp(s(\bar{x} - h_+) + m) \approx 0$.

Now that an appropriate normalization technique is available, preprocessing can proceed. First, the dataset is created for a given availability parameter b , and missing records are stored in $\mathbb{X}^{\text{missing}}$. Then, the remaining data is split into training, validation and test sets with a ratio of 8:2:2. This splitting process is illustrated in Fig. 5. Note that the sizes of these datasets also depend on the selected b . Then, the zero-preserved log-normalization ($h_0=-3$, $h_+=1$) is applied to each feature, $x^{(t)}$, individually. Note that the zero-excluded mean $m^{(t)}$ and standard deviations $s^{(t)}$ are estimated using only the training set but applied to all sets.

3) *Conditioning*: As mentioned in Section III-C, there are two main components of the conditions (\mathbf{c}_{un}) used in the GUIDE-VAE training: the sampled user vector $\hat{\theta}_u$, and the auxiliary condition vector $\tilde{\mathbf{c}}_{un}$. The generation of user dictionary Γ to take user vector samples is explained thoroughly in Sections II-B and III-A. Similar to the normalization step, only the training data is used in LDA-based user embedding, and the resulting dictionary Γ is stored for a given user embedding hyper-parameter combination (W , K). The prior parameters always kept equal to $\eta = \frac{1}{W}$ and $\alpha = \frac{1}{K}$.

It is decided to conduct the experiments using two auxiliary conditions: months and weekdays. These conditions are extracted using the data index n , encoded using the cyclic (sin-cos) transformation like in [19], and assigned to their respective data points \mathbf{x}_{un} . Due to the inherited seasonality, we believe these are essential for energy consumption time series modelling.⁷

B. Training

1) *Neural networks*: The neural network structure used in the experiments, both for the encoder and decoder, is depicted in Fig. 7. As can be seen, the input size ($T + K + 4$) is the same for both of the networks. This is because the size of the latent space is fixed to $T=24$ in all experiments since the main objective is data modelling, not dimensionality reduction. The remaining part of the input ($K+4$) comes from the conditions. The only part that differs between the two networks is the output size of the Output Layer ($\sigma/\tilde{\sigma}$), which equals T for the encoder and V for the decoder. Lastly, L and M are set to 3 and 1000, respectively, for all experiments.

⁶Please note that the zero-preserved log-normalization differs from the conventional offsetting ($\bar{x}_i = x_i + \delta$, $\forall i \in [N]$) and zero-replacement ($\bar{x}_i = \delta$, $\forall i \in \mathbb{I}_0$) by excluding zeros from the estimation of m and s , so that they are not affected by the unwanted skewness comes with the zeros.

⁷Since the aim is not finding the best generative model but showcasing the benefits of GUIDE-VAE, the number of auxiliary conditions is limited to two.

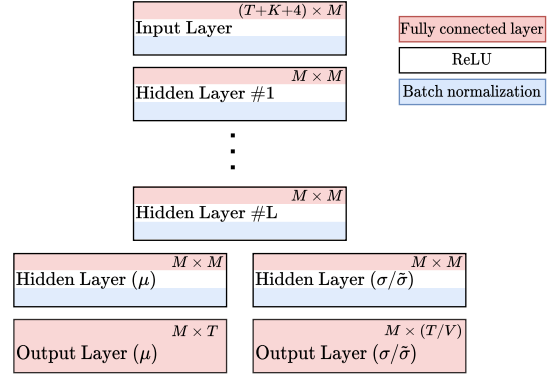


Fig. 7. The neural network architecture used both for encoder and decoder.

2) *Constraints*: There are various constraints on the outputs of both the encoder and decoder for numerical stability. Firstly, the base variance ξ is set to 10^{-2} , which means the marginal standard deviations of the likelihood distribution are bounded below by 10^{-1} . Similarly, this bound for the posterior distribution is set to 5×10^{-1} . Likewise, the mean parameters of both distributions are constrained between -3 and 5, causing better convergence without hurting the modelling performance.

3) *Optimization*: Adam [20] is used for the optimization of the GUIDE-VAE with its default parameters⁸, and L2-regularization is applied over all parameters (including \mathbf{U}) with a coefficient of 10^{-5} . Moreover, an adaptive learning rate scheduler and early stopping are applied using the validation set to further prevent overfitting. Lastly, $N^{\text{MC}}=16$ is used for Monte Carlo sampling that appears in the ELBO objective.

C. Performance metric

In order to assess the performance of the trained generative models, two datasets are used: \mathbb{X}^{test} for the synthetic data generation and $\mathbb{X}^{\text{missing}}$ for the imputation performance. The log-likelihood of a given set on the generative models

$$\mathbb{E}_{p.(\mathbf{x}, \mathbf{c})} [\log p_\psi(\mathbf{x}|\mathbf{c})] = \frac{1}{|\mathbb{X}|} \sum_{\mathbf{x}_{un} \in \mathbb{X}} \log p_\psi(\mathbf{x}_{un}|\mathbf{c}_{un}) \quad (14)$$

is chosen as the performance metric. Here $p.(\mathbf{x}, \mathbf{c})$ is the empirical distribution representing either the testing or missing datasets and their respective conditions. Since $\log p_\psi(\mathbf{x}_{un}|\mathbf{c}_{un})$ is intractable, it is approximated by the importance sampling as

$$\begin{aligned} \log p_\psi(\mathbf{x}_{un}|\mathbf{c}_{un}) &= \log \mathbb{E}_{q_\phi} \left[\frac{p_\psi(\mathbf{x}_{un}, \mathbf{z}|\mathbf{c}_{un})}{q_\phi(\mathbf{z}|\mathbf{x}_{un}, \mathbf{c}_{un})} \right] \\ &\approx -\log S^{\text{MC}} + \log \sum_{s=1}^{S^{\text{MC}}} \frac{p_\psi(\mathbf{x}_{un}|\hat{\mathbf{z}}_{uns}, \hat{\theta}_{us}, \tilde{\mathbf{c}}_{un}) p(\hat{\mathbf{z}}_{uns})}{q_\phi(\hat{\mathbf{z}}_{uns}|\mathbf{x}_{un}, \hat{\theta}_{us}, \tilde{\mathbf{c}}_{un})} \end{aligned} \quad (15)$$

where $\{\hat{\mathbf{z}}_{uns}\} \stackrel{S^{\text{MC}}}{\sim} q_\phi(\mathbf{z}|\mathbf{x}_{un})$ and $\{\hat{\theta}_{us}\} \stackrel{S^{\text{MC}}}{\sim} \text{Dir}(\gamma_u)$. After sweeping different values, we set $S^{\text{MC}}=100$ for all the experiments to balance the computational time for testing and estimation variance.

⁸ $\beta_1=0.9$, $\beta_2=0.999$.

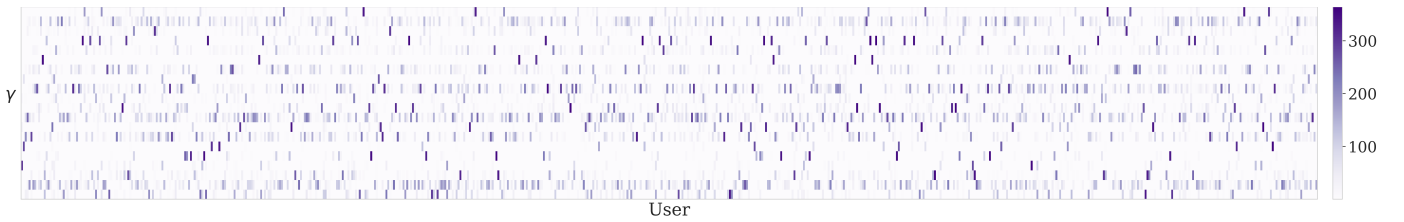


Fig. 8. A learned user dictionary Γ with $K=20$.

Please note that the conventional sample comparison-based performance metrics are inadequate for this task since they require preferably a larger sample population to represent the distribution to compare. Unfortunately, the number of samples for a given condition tends to be very limited when the conditions get plenty. For instance, the dataset used in this study has three conditions: users, months and weekdays. This means there are at most five instances of a given condition triplet in a year-long dataset, and they are far from effectively representing a conditional distribution. This problem gets even more severe when continuous conditions are employed.

V. RESULTS

The results of the experiments that were conducted are showcased here. The following hyper-parameter values are used as default unless it is stated otherwise:

- Data availability rate: $b = 10$
- User vector size: $K = 100$
- Pattern dictionary size: $V = 100$
- Wording granularity: $W = 1000$
- Auxillary standard deviation lower-bound: $\varepsilon = 10^{-4}$
- Marginal variance lower-bound: $\xi = 10^{-2}$

These default values were selected based on preliminary tuning to balance computational efficiency and performance.

A. Visual inspection

The user and pattern dictionaries and generated time series samples after training are visualized in this section. We start the visualization by showing a 20-dimensional ($K=20$) user dictionary Γ in Fig. 8 as the output of the user embedding scheme.⁹ The visual inspection suggests that the user vectors are dispersed enough to capture discrepancies between user behaviours.

Next, we investigate the pattern dictionaries of two GUIDE-VAE models with $V=25$ and $V=100$. For better visualization, the pattern vectors (\mathbf{u}_v) are sorted with respect to their L_1 -norm, and the resulting matrices are given in Fig. 9. One can immediately spot the richness of patterns coming with the increasing dictionary size, which is expected since it allows GUIDE-VAE to exploit finer details and more intrinsic correlations between time steps. For instance, a large variety of switching behaviours are captured by the model on the right side of the dictionary in Fig. 9b, which are absent in Fig. 9a.

Lastly, we visualize the data generated by GUIDE-VAE with varying dictionary sizes. For this, we conducted a sub-experiment in which we selected a random user u' from the

dataset, and we imputed its missing time series, $\mathbb{X}_{u'}^{\text{missing}} = \mathbb{X}^{\text{missing}} \cap \mathbb{X}_{u'}$, 10^4 times by sampling $\{\hat{\mathbf{z}}_{ns}\}_s \stackrel{10^4}{\sim} p(\mathbf{z})$, $\forall n$ and $\{\hat{\theta}_s\} \stackrel{10^4}{\sim} \text{Dir}(\gamma_{u'})$. Note that each sample s from the prior distribution corresponds to a likelihood distribution, and we aim to visualize the samples from these likelihood distributions, $\hat{\mathbf{x}}_{ns} \sim p_\psi(\mathbf{x}_n | \hat{\mathbf{z}}_{ns}, \hat{\theta}_s, \hat{\mathbf{c}}_n)$, since these are the final outcomes during inference. For visualization we concatenated the profiles of a given sample s as $\hat{\mathbf{x}}_s = [\hat{\mathbf{x}}_{ns}]_{n=1}^{M_{u'}} \in \mathcal{X}^{M_{u'}T}$, where $|\mathbb{X}_{u'}^{\text{missing}}| = M_{u'}$. The resulting samples for each model are given in Fig. 10. In order to showcase the typical performance of each model, we calculated the log-likelihood of the ground truth time series on each sampled distribution, i.e. $\sum_{\mathbf{x}_n \in \mathbb{X}_{u'}^{\text{missing}}} \log p_\psi(\mathbf{x}_n | \hat{\mathbf{z}}_{ns}, \hat{\theta}_s, \hat{\mathbf{c}}_n)$, $\forall s$, and found the sample that corresponds to median (5×10^3 -th highest) of these scores. This ‘‘median best sample’’ is also given in Fig. 10.

As can be seen from Fig. 10, all models can generate samples that are very close to the ground truth. Please note that these were generated using only the user embedding, month, and weekday information pieces. Also, recall that the ground truth profile was never seen in the training. This showcases the generalization power of GUIDE-VAE. Another qualitative outcome of this experiment is the plausibility of the generated samples. As one can see, not only the median ones but all samples get less noisy with the increasing pattern dictionary size. We claim that the larger the pattern dictionary, the more likely it is to observe realistic samples.

B. Effect of user embeddings

In order to analyse the effect of user embeddings, two independent hyper-parameter sweeps are considered:

- $K \in \{0, 5, 10, 20, 50, 100\}$
- $W \in \{0, 250, 500, 1000, 2000\}$

The results of the user vector size K and wording granularity W sweeps are given in Fig. 11 and 12, respectively.

The first and the most obvious conclusion from Fig. 11 is that the introduction of user embeddings boosts the performance considerably. This showcases the importance of using user information in modelling multi-user datasets. Furthermore, it can be seen that the performance improvement is nearly monotonic with the increasing K . This makes sense since the higher the user vector dimensionality, the more information can be conveyed to GUIDE-VAE. We see that this is subject to saturation after some K values. Practitioners can select among these values to not overwhelm the input sizes of the neural networks with unnecessarily large user vectors.

⁹Here, only 10% of the users are given due to visibility concerns.

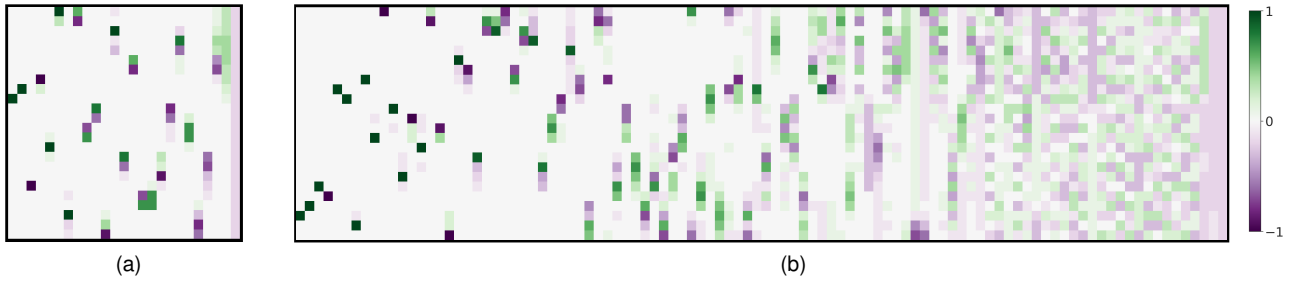


Fig. 9. Pattern dictionaries \mathbf{U} from two trained GUIDE-VAE models with (a) $V=25$ and (b) $V=100$, sorted according to L_1 -norm of the pattern vectors.

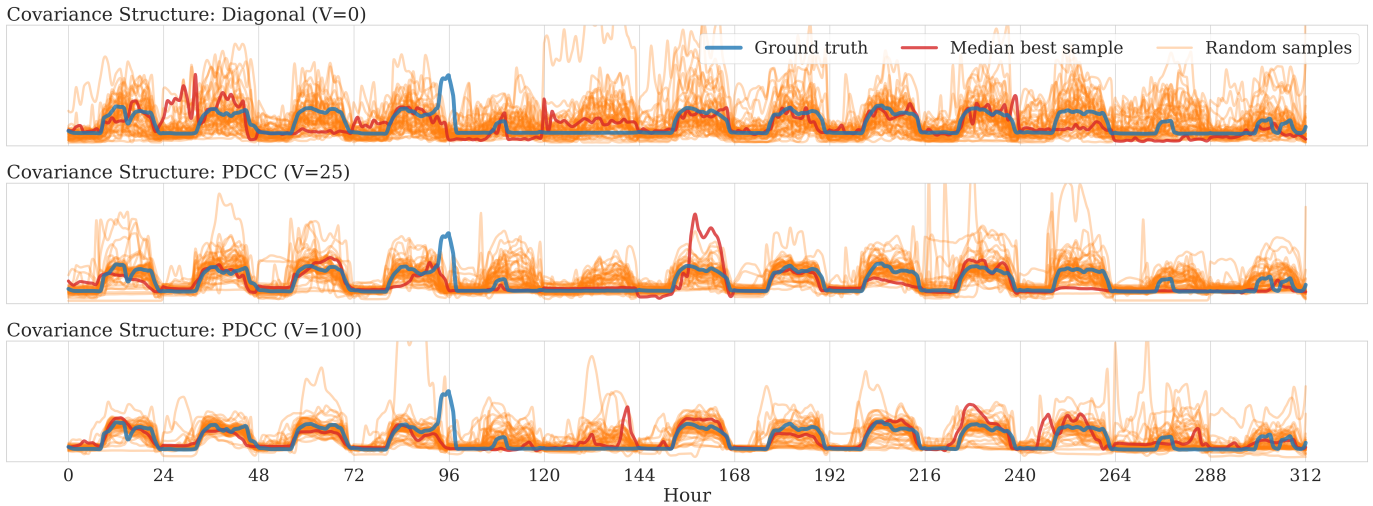


Fig. 10. The effect of pattern dictionary size V on the sample quality. A selected user’s missing time series measurements (in blue) and the 10 closest imputations (in red) out of 1000 generated time series (50 of which are in orange).

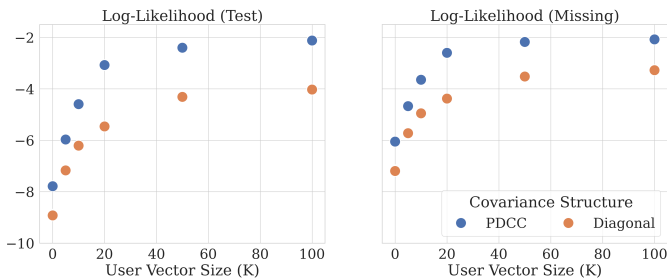


Fig. 11. The effect of user vector size K on the modelling performance. $K=0$ means no conditioning on users.

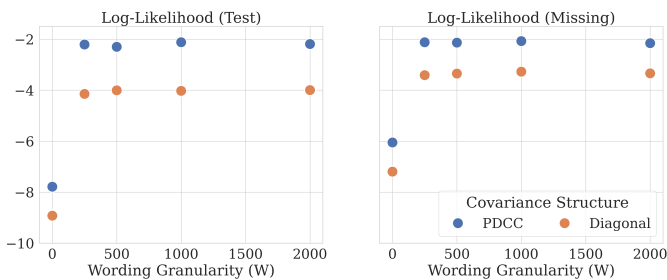


Fig. 12. The effect of wording granularity W on the modelling performance. $W=0$ means no conditioning on users.

On the other hand, Fig. 12 reveals that cluster sizes above 250 are merely effective on the performance of this dataset. Since this is a computationally light step of the user embedding scheme and does not affect the input sizes of the neural networks, moderately high granularities can be used for wording.

Another result given in these figures is the performance improvement that comes with PDCC. As one can see, using a pattern dictionary with size $V = 100$ consistently increases the performance over a diagonal covariance structure. This shows that GUIDE-VAE brings out significant performance improvements by utilizing both of the proposed methods.

We also showcase that this performance improvement not only comes at the global level but also at the user level by calculating the log-likelihood scores individually for each user. We conducted this experiment with a user-guided ($K=100$) and an unguided model by calculating the log-likelihood scores of individual testing ($\mathbb{X}_u^{\text{test}} = \mathbb{X}^{\text{test}} \cap \mathbb{X}_u$) and missing datasets ($\mathbb{X}_u^{\text{missing}} = \mathbb{X}^{\text{missing}} \cap \mathbb{X}_u$). Then, we subtracted the individual unguided scores from the guided ones and called the resulting differences “log-likelihood gain per user”. The resulting histograms for both sets are given in Fig. 13. We can see that introducing user embeddings boosts the modelling of certain users significantly more than others. However, the negative values in the log-likelihood gain on the missing set imply that out-of-distribution generalization is not guaranteed with GUIDE-VAE.

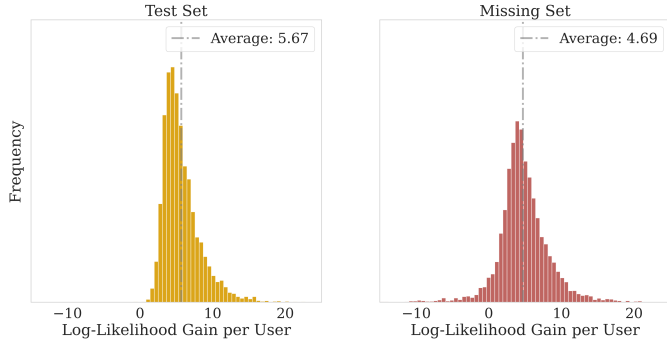


Fig. 13. Distributions of log-likelihood gains come with conditioning on user embeddings, per user.

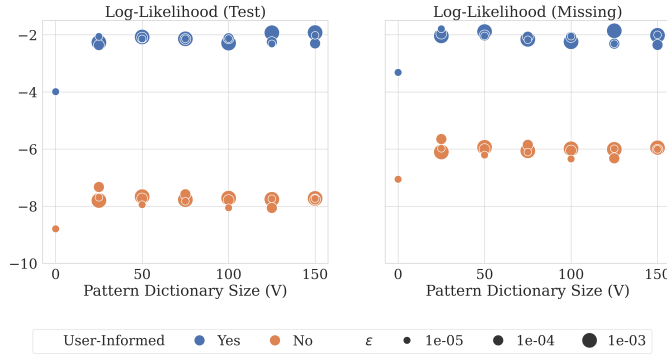


Fig. 14. The effect of pattern dictionary size V on the modelling performance. $V=0$ corresponds to a diagonal covariance matrix.

C. Effect of PDCC

Two hyper-parameter value sets for the pattern dictionary size V and the lower-bound ϵ are set as

- $V \in \{0, 25, 50, 75, 100, 125, 150\}$
- $\epsilon \in \{10^{-5}, 10^{-4}, 10^{-3}\}$

and a sweep conducted on their product set, i.e. all the possible V and ϵ combinations are tested. Like before, a value of 0 means no employment of PDCC, i.e. a diagonal covariance matrix structure. In these cases, ϵ does not refer to anything.

The results of this sweep are given in Fig. 14. As mentioned before, the performance improvement that comes with PDCC is apparent. On the other hand, we see that the selection of neither the dictionary size nor the lower bound causes a significant change in the performance. Please recall that the main motivation for proposing PDCC was to introduce more realism to the generated samples. will be investigated in the qualitative results sections.

A natural question that arises is why a larger dictionary size does not affect the performance significantly if it means higher representative power, as we claimed before. To answer this, we must investigate the two components of ELBO given in (5), namely the reconstruction log-likelihood and Kullback-Leibler divergence. These two metrics were calculated for trained models with varying V , and the results are given in Fig. 15. As can be seen, increasing the dictionary size results in a decrease both in reconstruction and Kullback-Leibler divergence. It indicates that the pattern dictionary undertakes the representation burden from the latent space. This can also

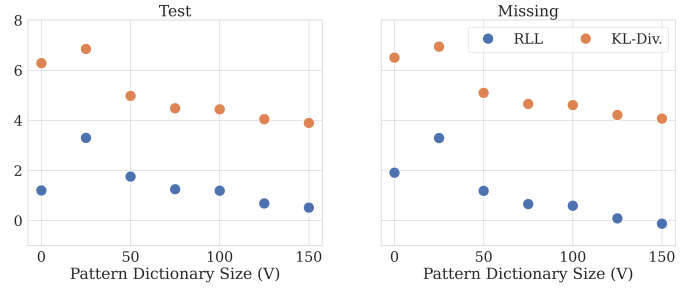


Fig. 15. The effect of pattern dictionary size V on reconstruction log-likelihood (RLL) and Kullback-Leibler divergence (KL-Div). $V=0$ corresponds to a diagonal covariance matrix.

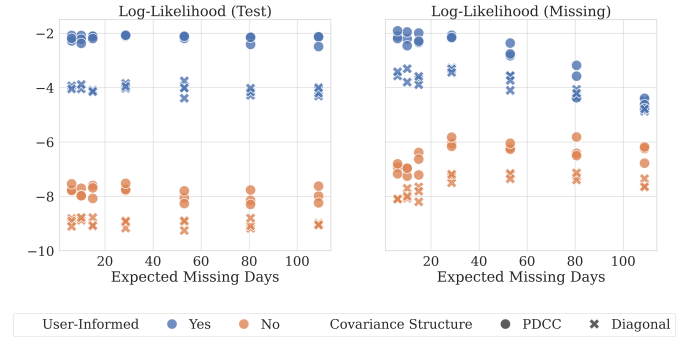


Fig. 16. The effect of expected missing days (controlled by b) on the modelling performance.

be observed from the decreasing deviation on the samples with the pattern dictionary size in Fig. 10. In other words, the model gets more confident about the likelihood distribution imposed by the conditions, and the latent variable \mathbf{z} poses a minimal effect on generation. In other words, a large pattern dictionary results in a more consistent sampling process.

D. Effect of missingness

Lastly, we investigate the effect of the missing set size to the performance by sweeping the data availability rate b as

- $b = \{2, 3, 5, 10, 20, 30, 50\}$

which corresponds to a series of expected missing days per user calculated as $\mathbb{E}[M_u] = 365 \frac{0.85}{0.85+b}$. Since this amputation process is conducted at the very beginning of the entire training pipeline and is inherently stochastic, relying on a single amputation scenario can be fallacious. Thus, this process is repeated three times with different random number generator kernels for each hyper-parameter configuration.

The experiment results with respect to the expected number of missing days are given in Fig. 16. One can immediately spot the near monotonic decline in the performance with expected missing days on the missing set when the user embeddings are provided while still being superior to its unguided counterparts. On the other hand, the performance on the testing set appears to be robust to the training data size. This is expected since the testing set is a fixed portion (20%) of the non-missing part, and the training data is abundant enough ($\sim 1M$, at worst) to “interpolate”.

The robust behaviour in testing performance suggests that GUIDE-VAE can be used confidently for synthetic data generation tasks even under severe missingness. Unfortunately, this is not the case for the imputation performance since the missingness is biased toward the first days of the year. The increasing number of missing days per user creates a vacuum of ignorance about these periods, and the improved modelling capacity that comes with user embeddings inhibits the out-of-distribution generalization power of GUIDE-VAE. Thus, we advise practitioners to use GUIDE-VAE cautiously for the extrapolative missing value imputation tasks.

VI. CONCLUSION

In this work, we introduced GUIDE-VAE, a novel framework for generating realistic and user-guided time series data in multi-user settings. First, we proposed probabilistic user embeddings as conditions for generative models, which can be applied to any conditional generative model. This approach effectively addresses the challenges of user-agnostic data generation and data imbalance by incorporating user identities, leading to significant performance improvements. Second, we introduced PDCC to enhance the realism of generated data, particularly by VAEs. PDCC mitigates the common issue of noisy outputs, allowing the model to capture complex feature dependencies and generate realistic time series data.

We combined these contributions in the GUIDE-VAE model and demonstrated its effectiveness on a multi-user smart meter dataset. We considered two tasks, namely synthetic data generation and missing records imputation, and the results showed significant improvements over conventional CVAE models, both in modelling performance and sample quality. In overall, GUIDE-VAE offers a powerful solution for generating realistic and user-guided data.

As future work, we plan to showcase the effect of user embeddings in other conditional generative models. Also, we desire to investigate other applications such as forecasting. Lastly, we plan to apply GUIDE-VAE on other multi-use datasets like healthcare and finance.

REFERENCES

- [1] Z. Qian, T. Callender, B. Cebere, S. M. Janes, N. Navani, and M. van der Schaar, "Synthetic data for privacy-preserving clinical risk prediction," *medRxiv*, pp. 2023–05, 2023.
- [2] X. Peng, S. Luo, J. Guan, Q. Xie, J. Peng, and J. Ma, "Pocket2mol: Efficient molecular sampling based on 3d protein pockets," in *International Conference on Machine Learning*. PMLR, 2022, pp. 17 644–17 655.
- [3] J. Yoon, L. N. Drumright, and M. Van Der Schaar, "Anonymization through data synthesis using generative adversarial networks (ads-gan)," *IEEE journal of biomedical and health informatics*, vol. 24, no. 8, pp. 2378–2388, 2020.
- [4] D. P. Kingma, "Auto-encoding variational bayes," *arXiv preprint arXiv:1312.6114*, 2013.
- [5] K. Sohn, H. Lee, and X. Yan, "Learning structured output representation using deep conditional generative models," *Advances in neural information processing systems*, vol. 28, 2015.
- [6] G. Bredell, K. Flouris, K. Chaitanya, E. Erdil, and E. Konukoglu, "Explicitly minimizing the blur error of variational autoencoders," *arXiv preprint arXiv:2304.05939*, 2023.
- [7] S. Chai, G. Chadney, C. Avery, P. Grunewald, P. Van Hentenryck, and P. L. Donti, "Defining 'good': Evaluation framework for synthetic smart meter data," *arXiv preprint arXiv:2407.11785*, 2024.

- [8] C. Sun, J. van Soest, and M. Dumontier, "Generating synthetic personal health data using conditional generative adversarial networks combining with differential privacy," *Journal of Biomedical Informatics*, vol. 143, p. 104404, 2023.
- [9] S. Zhang, L. Yao, A. Sun, and Y. Tay, "Deep learning based recommender system: A survey and new perspectives," *ACM computing surveys (CSUR)*, vol. 52, no. 1, pp. 1–38, 2019.
- [10] X. Chen, C. Zanocco, J. Flora, and R. Rajagopal, "Constructing dynamic residential energy lifestyles using latent dirichlet allocation," *Applied Energy*, vol. 318, p. 119109, 2022.
- [11] A. J. Almansoori, S. Horváth, and M. Takáč, "Padpap: Partial disentanglement with partially-federated gans," 2022.
- [12] D. M. Blei, A. Y. Ng, and M. I. Jordan, "Latent dirichlet allocation," *Journal of machine Learning research*, vol. 3, no. Jan, pp. 993–1022, 2003.
- [13] B. Van Breugel, T. Kyono, J. Berrevoets, and M. Van der Schaar, "Decaf: Generating fair synthetic data using causally-aware generative networks," *Advances in Neural Information Processing Systems*, vol. 34, pp. 22 221–22 233, 2021.
- [14] S. Hans, A. Sanghi, and D. Saha, "Tabular data synthesis with gans for adaptive ai models," in *Proceedings of the 7th Joint International Conference on Data Science & Management of Data*, 2024, pp. 242–246.
- [15] G. Dorta, S. Vicente, L. Agapito, N. D. F. Campbell, and I. Simpson, "Structured uncertainty prediction networks," in *Proceedings of the IEEE Conference on Computer Vision and Pattern Recognition (CVPR)*, June 2018.
- [16] J. Langley, M. Monteiro, C. Jones, N. Pawlowski, and B. Glocker, "Structured uncertainty in the observation space of variational autoencoders," *Transactions on Machine Learning Research*, 2022.
- [17] K. Muandet, K. Fukumizu, B. Sriperumbudur, B. Schölkopf *et al.*, "Kernel mean embedding of distributions: A review and beyond," *Foundations and Trends® in Machine Learning*, vol. 10, no. 1-2, pp. 1–141, 2017.
- [18] C. Quesada, L. Astigarraga, C. Merveille, and C. E. Borges, "An electricity smart meter dataset of spanish households: insights into consumption patterns," *Scientific Data*, vol. 11, no. 1, p. 59, 2024.
- [19] C. Wang, S. H. Tindemans, and P. Palensky, "Generating contextual load profiles using a conditional variational autoencoder," in *2022 IEEE PES Innovative Smart Grid Technologies Conference Europe (ISGT-Europe)*, 2022, pp. 1–6.
- [20] D. P. Kingma, "Adam: A method for stochastic optimization," *arXiv preprint arXiv:1412.6980*, 2014.

APPENDIX A PROOFS

Theorem 1. *Any positive definite matrix can be constructed using PDCC at least in $V(V - T) + 1$ different ways.*

Proof. Let $\mathbf{M} \in \mathbb{R}^{T \times T}$ be a positive definite matrix with eigenvalues $\lambda_t > 0, \forall t$. Then, the Cholesky decomposition of $(\mathbf{M} - \xi \mathbf{I})$ results in a unique lower triangular matrix $\mathbf{L} \in \mathbb{R}^{T \times T}$ such that $\mathbf{M} - \xi \mathbf{I} = \mathbf{L}\mathbf{L}^\top$ as long as $\xi < \min(\{\lambda_i\})$. Thus, we shall perform the construction $\mathbf{L}\mathbf{L}^\top = \mathbf{U}\tilde{\Sigma}\mathbf{U}^\top$. Let us define $\mathbf{U} = [\mathbf{L} \ \mathbf{0}] \begin{bmatrix} \mathbf{Q} \\ \tilde{\mathbf{U}} \end{bmatrix}$ where $\mathbf{Q} = [\mathbf{Q}_\perp \ \tilde{\mathbf{Q}}]$. Here, $\mathbf{Q}_\perp \in \mathbb{R}^{T \times T}$ is orthogonal, and $\tilde{\mathbf{U}} \in \mathbb{R}^{(V-T) \times V}$ and $\tilde{\mathbf{Q}} \in \mathbb{R}^{T \times (V-T)}$ are free. Thus, by replacing \mathbf{U} , we obtain

$$\begin{aligned} \mathbf{L}\mathbf{L}^\top &= \mathbf{L}\mathbf{Q}\tilde{\Sigma}(\mathbf{L}\mathbf{Q})^\top + \mathbf{0}\tilde{\mathbf{U}}\tilde{\Sigma}(\mathbf{0}\tilde{\mathbf{U}})^\top \Rightarrow \mathbf{I} = \mathbf{Q}\tilde{\Sigma}\mathbf{Q}^\top \\ &\Rightarrow \mathbf{I} = \mathbf{Q}_\perp \tilde{\Sigma}_1 \mathbf{Q}_\perp^{-1} + \tilde{\mathbf{Q}} \tilde{\Sigma}_2 \tilde{\mathbf{Q}}^\top \end{aligned}$$

where $\begin{bmatrix} \tilde{\Sigma}_1 \\ \tilde{\Sigma}_2 \end{bmatrix} = \tilde{\Sigma}$. This equation always has at least one solution, e.g. $\tilde{\Sigma}_1 = \mathbf{I}, \tilde{\mathbf{Q}} = \mathbf{0}$. Therefore, M can be constructed at least $V(V - T) + 1$ different ways by choosing ξ and the elements of $\tilde{\mathbf{U}}$ independently. \square